

## Effect of Benzotriazole Derivatives on Steel Corrosion in Solution Simulated Carbonated Concrete

*Ayman Ababneh*<sup>1)</sup>, *Mashal Sheban*<sup>2)</sup>, *Muna Abu-Dalo*<sup>3)</sup> and *Silvana Andreescu*<sup>4)</sup>

<sup>1)</sup> Assistant Prof., Department of Civil Engineering, Jordan University of Science and Technology, P.O.Box 3030, Irbid 22110, Jordan, Phone (962-2) 7201000x 22121, Fax (962-2) 7201040, [anababneh@just.edu.jo](mailto:anababneh@just.edu.jo)

<sup>2)</sup> Assistant Prof., Department of Civil Engineering, Hadramout University of Science and Technology, P.O. Box (50512-50511), Mukalla, Yemen

<sup>3)</sup> Assistant Prof., School of Applied Natural Sciences, German-Jordanian University, P.O.Box 35247, Amman 11180 Jordan

<sup>4)</sup> Assistant Prof., Department of Chemistry, Clarkson University, P. O.Box 5810, Potsdam, NY 13699, Phone +1 315/268-2394, FAX 315/268-6610, [eandrees@clarkson.edu](mailto:eandrees@clarkson.edu)

### ABSTRACT

The aim of this research was to develop corrosion protection systems for reinforced concrete structures under carbonation attack. Benzotriazole (BTA) and BTA derivatives were used as two separate protection systems: inhibition and pickling protection systems. The experiments were performed in Simulated Concrete Pore (SCP) solutions with and without severe carbonation attack. Electrochemical techniques, i.e. potentiodynamic polarization and electrochemical impedance were used to assess the steel corrosion protection systems. The potentiodynamic polarization studies showed a reduction in the corrosion rate and a shifting in the corrosion potential to more noble potential for the steel specimen in the simulated carbonated concrete solution. In addition, a large increase in the steel interfacial resistance was observed by Electrochemical Impedance Studies (EIS) due to the formation of steel-BTA derivative complex on the surface. BTA derivatives provided a good protection for the steel in SCP simulated carbonated concrete solutions. This study indicates the applicability of these compounds for steel corrosion protection in reinforced concrete structures.

**KEYWORDS:** Concrete, Carbonation, Steel, Benzotriazole, Protection, EIS.

### INTRODUCTION

Corrosion of steel reinforcement is a major deterioration mechanism for concrete structures in cold, marine and industrial environments. Corrosion damage accelerates the aging of highway bridges, concrete pavements, parking structures, waterfront structures and water and wastewater treatment structures. This, in turn, shortens their remaining service life, requires expenditures for maintenance, repair or replacement,

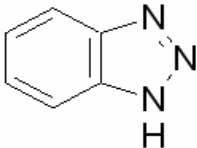
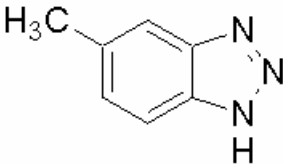
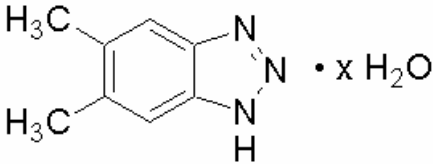
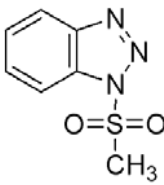
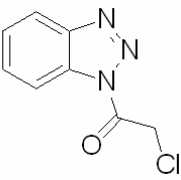
endangers the public safety and damages the environment. Corrosion of steel reinforcement is a major deterioration mechanism for the infrastructure systems worldwide.

In reinforced concrete, the formation of an oxide passive film on the steel surfaces protects the reinforcing bars (rebars) from corrosion. This film is stable and effectively prevents steel corrosion when the pH is greater than 11.5 (Benture et al., 1997). However, depassivation of that film and therefore an onset of active corrosion can arise in conjunction with two particular conditions: chloride and carbonation intrusion, or a combination

---

Accepted for Publication on 15/1/2009.

**Table (1): Names and molecular structures of the benzotriazole derivatives.**

Synonym	Abbr.	Molecular Formula	Molecular structure	Manufactured by
Benzotriazole	BTA	$C_6H_5N_3$		Alfa Aesar
5-Methyl-1H-Benzotriazole	MBTA	$C_7H_7N_3$		TCI America
5,6-Dimethyl-1H-Benzotriazole monohydrate	DMBTA	$C_8H_9N_3 \cdot H_2O$		Alfa Aesar
1-Methanesulfonyl-1H-Benzotriazole	MSBTA	$C_7H_7N_3O_2S$		Sigma-Aldrich Co.
1-(alpha-Chloroacetyl)-1H-Benzotriazole	CABTA	$C_8H_6ClN_3O$		Sigma-Aldrich Co.

of both. The chloride attack arises in conjunction with deicing activities or from coastal exposure. The presence of chloride ions above a specified threshold level depassivates the protective film of the steel, initiating the pitting corrosion (Saremi and Mahallati, 2002; Xi and Ababneh, 2000). On the other hand, in the carbonation attack, atmospheric carbon

dioxide ( $CO_2$ ) penetrates into concrete and reacts with pore solution alkali and calcium hydroxide; these reactions cause a drastic drop in the alkalinity of the pore solution to levels of about pH 8 (Hartt et al., 2004). Under this low alkalinity, the passive film of the steel is destroyed and a uniform corrosion starts. The carbonation-induced corrosion is

common in urban and industrial areas where carbon dioxide exists in high ratio. In addition, the supplementary cementitious material, e.g. fly ash and silica fume, frequently used in concrete mixing in recent years accelerates the carbonation-induced corrosion (Montemor et al., 2002; Haque and Kawamura, 1993).

**Table (2): Polarization results obtained with control SCP solutions.**

Control	$E_{corr}$ (mV)	Corr. Rate ( $\mu\text{m}/\text{y}$ )
Blank 1 Ca(OH) <sub>2</sub> solution No attack	-231	1.05
Blank 2 Carbonation attack pH=8	-543	272

**Table (3): Protection efficiencies for BTA derivatives for the corrosion of steel in SCP solutions under carbonation attack with pickling protection system.**

Pickling Materials	$E_{corr}$ (mV)	Corr. Rate ( $\mu\text{m}/\text{y}$ )	Protection efficiency (PE%)
BTA	-492	62	77
MBTA	-492	80	71
DMBTA	-500	100	63
MSBTA	-492	100	63
CABTA	-477	75	72

A few studies on corrosion inhibitors have focused on steel in carbonated concrete environments. Among these, Alonso et al. (1996) tested Na<sub>2</sub>PO<sub>3</sub>F in simulated concrete pore solution under carbonated attack and in mortar specimens. Their results showed a significant reduction of the steel corrosion rate. Two organic bases (ethanolamine and guanidine) were tested as corrosion inhibitors for carbonated concrete by Sawada et al. (2005) using electrochemical injection. However, the corrosion rate and the inhibition efficiency were not evaluated. TrabANELLI et al. (2005) found that benzoic acid and amino benzoic acid can be used as corrosion inhibitors for carbonated concrete. Various other inhibitors such as sodium nitrite (Andrade et

al., 1986) and aminoalcohol-based inhibitors (Burge, 2000; Batis et al., 2003) have also been reported in literature to protect steel rebars in carbonated concrete. On-going research looks for new materials that can be used as inhibitors or protective coatings to provide more efficient protection for steel rebar in carbonated concrete.

Benzotriazole (BTA) and its derivatives are organic inhibitors known as the best corrosion inhibitors for copper and its alloys in acid and NaCl media (Ravichandran et al., 2004; Bastidas, 2006; Zhang et al., 2006; Abdullah et al., 2006). Benzotriazole and many of its derivatives, form very strong complexes with transition metals and are the most widely used types of corrosion inhibitors. Benzotriazole and its derivatives are most widely used as corrosion inhibitors for copper, copper-containing alloys and other “yellow” metals. Benzotriazoles are also used in aircraft and roadway deicing fluids, antifreeze, brake fluids, lubricating oils and industrial cooling systems. It is known that BTAs bind strongly to metals by forming bonds via the triazole ring. The resulting layer has shown remarkable resistant properties against corrosion, although the protective film is only of the order of molecular dimension (Hosseini et al., 2003). This film acts as a protective barrier that reduces transport of corrosive elements to the metal surface. The effects of five different BTA derivatives on the corrosion resistance properties of steel rebar under chloride attack were studied by Sheban et al. (2007). It was found that BTA derivatives form a surface complex between triazolic nitrogen atoms and steel surface. This BTA-steel complex enhances the steel properties against corrosion, but their tests were conducted only under chloride attack. Therefore, the effect of BTA derivatives on the corrosion resistance properties of steel rebar under carbonation attack is required in order to suggest their use in concrete structures.

The aim of this work was to investigate the effect of BTA and four BTA derivatives on the corrosion resistance properties of steel rebar in solutions simulating the concrete pore solution under carbonation attack. The carbonated concrete was simulated by saturated calcium hydroxide, Ca(OH)<sub>2</sub>, with pH equal to 8. Potentiodynamic polarization and electrochemical AC impedance techniques were used for the corrosion study.

**MATERIALS AND TEST METHODS****Steel Rebar**

Test specimens were cut from steel rebar grade 60 (ASTM A615) which is currently used as concrete reinforcement. The chemical composition was 0.42% C; 1.040% Mn; 0.180% Si; 0.033% P; 0.065% S; 0.450%

Cu; 0.150% Ni; 0.240% Cr; 0.029% Mo; 0.025% Sn; 0.005% V, 0.003% Ti; 0.002% B; balance Fe. The specimen surfaces were polished using a series of silicon carbide papers of grades #120 to #1500. Finally, the specimens were washed thoroughly with di-ionized water, degreased with acetone and dried.

**Table (4): Protection efficiencies for BTA derivatives for the corrosion of steel in SCP solutions under carbonation attack with inhibition protection system.**

Protection Materials	$E_{corr}$ (mV)	Corr. Rate ( $\mu\text{m}/\text{y}$ )	Protection efficiency (PE%)
BTA	-499	194	40
MBTA	-513	43	84
DMBTA	-483	42	85
MSBTA	-502	42	85
CABTA	-490	86	68

**Table (5): Impedance measurements and inhibition efficiency for BTA derivatives of the steel in SCP solutions under carbonation attack with pickling protection system.**

Protection Materials	$R_s$ (ohm.cm <sup>2</sup> )	$R_s+R_f+R_{ct}$ (ohm.cm <sup>2</sup> )	$R_f+R_{ct}$ (ohm.cm <sup>2</sup> )	$C_i$ (nF/cm <sup>2</sup> )	Protection efficiency (PE%)
No Protection	25	2500	2475	0.3223	--
BTA	25	3750	3725	0.2142	34
MBTA	12	3500	3488	0.0910	29
DMBTA	21	4125	4104	0.0774	40
MSBTA	19	4670	4651	0.0542	47
CABTA	15	4050	4035	0.0990	39

**Table (6): Impedance measurements and protection efficiency for BTA derivatives of the steel in SCP solutions under carbonation attack with inhibition protection system.**

Protection Materials	$R_s$ (ohm.cm <sup>2</sup> )	$R_s+R_f+R_{ct}$ (ohm.cm <sup>2</sup> )	$R_f+R_{ct}$ (ohm.cm <sup>2</sup> )	$C_i$ (nF/cm <sup>2</sup> )	Protection efficiency (PE%)
No Protection	25	2500	2475	0.3223	--
BTA	25	5700	5675	0.0280	56
MBTA	25	5025	5000	0.0401	51
DMBTA	25	4900	4875	0.0206	49
MSBTA	75	6475	6400	0.0157	61
CABTA	20	5900	5880	0.0086	58

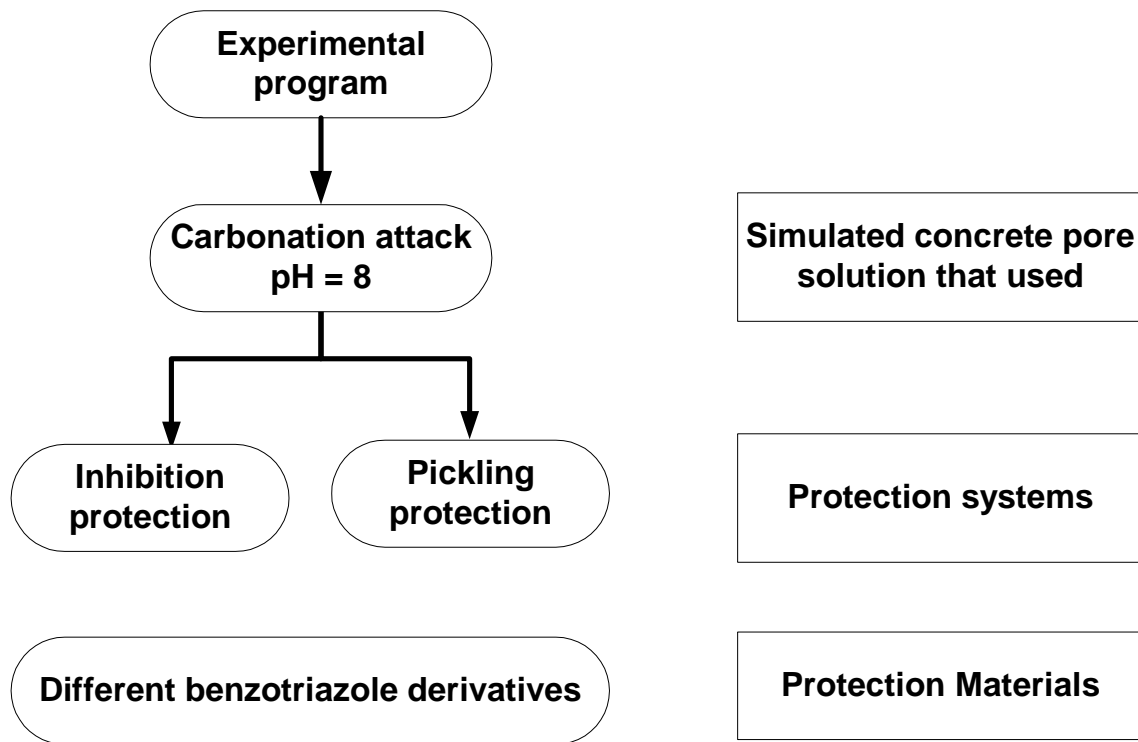


Figure (1): Schematic diagram of the experimental approach.

#### Simulated Concrete Pore Solution

In this work, only the concrete under carbonation attack was simulated. Saturated calcium hydroxide,  $\text{Ca}(\text{OH})_2$ , with a pH equal to 12.5 was used to simulate the concrete pore solution with no attack; to simulate the carbonation attack where the pH in pores reaches 8, the pH of the saturated calcium hydroxide,  $\text{Ca}(\text{OH})_2$ , is adjusted by hydrochloric acid (HCl) to pH equal to 8.

#### Protection Systems and Materials

Five different BTA derivatives were used in this research to study the influence of the various functional groups on BTA in the corrosion protection of steel in concrete. The molecular structures of BTA derivatives and the manufacturer are shown in Table (1). Each BTA derivative was used in two different protection systems (inhibition and pickling), and the effectiveness of each system in protecting the steel rebar under carbonation attacks was tested (see Figure 1). The inhibition protection system used BTA derivatives as inhibitors

which were added to the Simulated Concrete Pore (SCP) solutions before the corrosion tests began. In the pickling system, the steel specimens were incubated in 0.005 M BTA derivative solutions saturated with  $\text{Ca}(\text{OH})_2$  for 15 hours. The optimum experimental conditions were selected based on the previous study (Sheban et al., 2007). After the steel specimens were removed from the pickling solutions, corrosion tests were conducted in the SCP solutions.

#### Potentiodynamic Polarization Studies

The polarization measurements were carried out in a conventional electrochemical cell (200 ml) with three electrodes, i.e., reference, counter and working electrodes. A Saturated Calomel Electrode (SCE) was used as reference electrode, and all potentials were referred vs. the SCE. Also, a Luggin bridge tube was used to minimize ohmic resistance interference (Jones, 1996). A platinum wire was used as counter electrode. The working electrode was a cylindrical steel specimen with a

geometrical area of 4 cm<sup>2</sup>, prepared from the steel rebar as mentioned previously. The anodic and cathodic polarization curves were obtained after the working electrode was immersed in the test solution for 130 minutes, when stabilization was achieved. Then, the polarization was scanned from a potential 250 mV more

negative to the Open Circuit Potential (OCP) of each specimen toward 250 mV more positive to the OCP, with a constant potential scan rate of 0.125 mV/sec. A Gamry potentiostat (model PCI4/300) was used to carry out the tests, and the data were analyzed using the Gamry Echem Analyst software version 1.35.

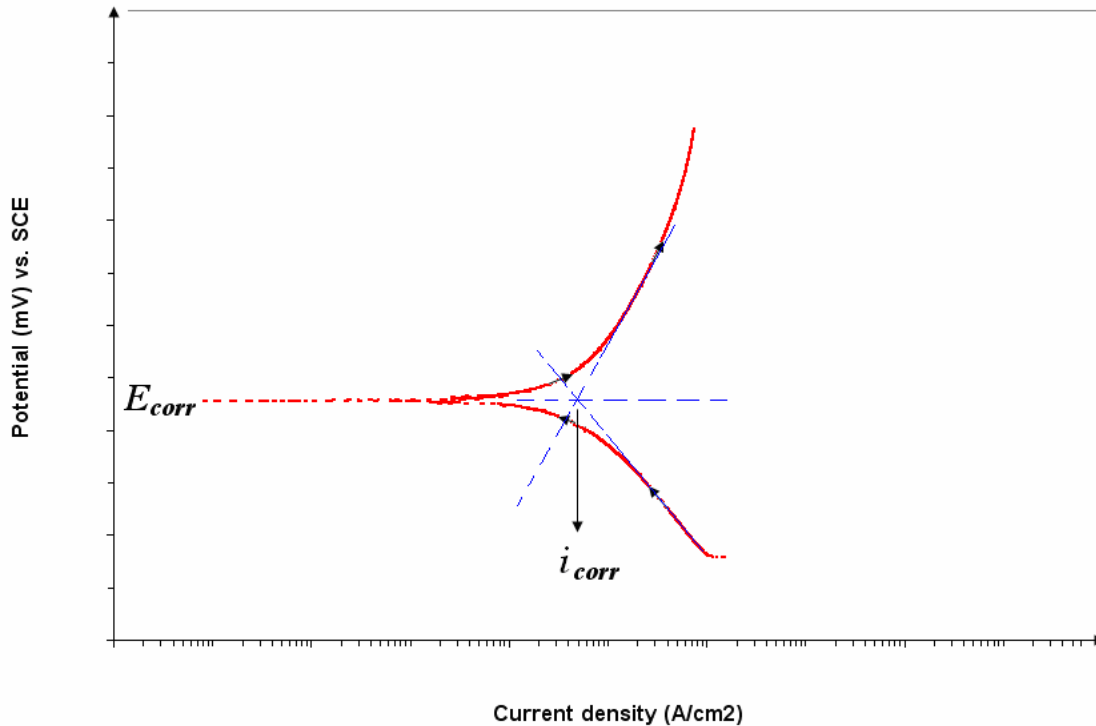


Figure (2): Schematic diagram of potentiodynamic polarization for steel in SCP solution.

### Electrochemical Impedance Studies

The Electrochemical A.C. Impedance Spectra (EIS) tests were carried out using the same three-electrode set-up and the same conditions as the ones used for the potentiodynamic polarization tests. Measurements were made using a potentiostat model PARSTAT 2263 and PowerSINE v. 2.46 Electrochemical Interface. The measurements were recorded at the corrosion potential by applying a  $\pm 10$  mV sine wave in a frequency range from 100 kHz to 2 MHz. The film resistance,  $R_f$ , and the charge transfer resistance,  $R_{ct}$ , were calculated from the

impedance spectra and the results were used to evaluate the protection efficiency. The protection efficiency,  $PE\%$ , based on EIS tests was calculated as follows:

$$PE\% = \frac{R_b^{-1} - R_{ps}^{-1}}{R_b^{-1}} * 100, \quad (1)$$

where  $R$  is the summation of the film resistance,  $R_f$ , and charge transfer resistance,  $R_{ct}$ . The subscript  $b$  refers to the resistance in a blank solution with no protection system, and the subscript  $ps$  refers to the resistance in a protective system.

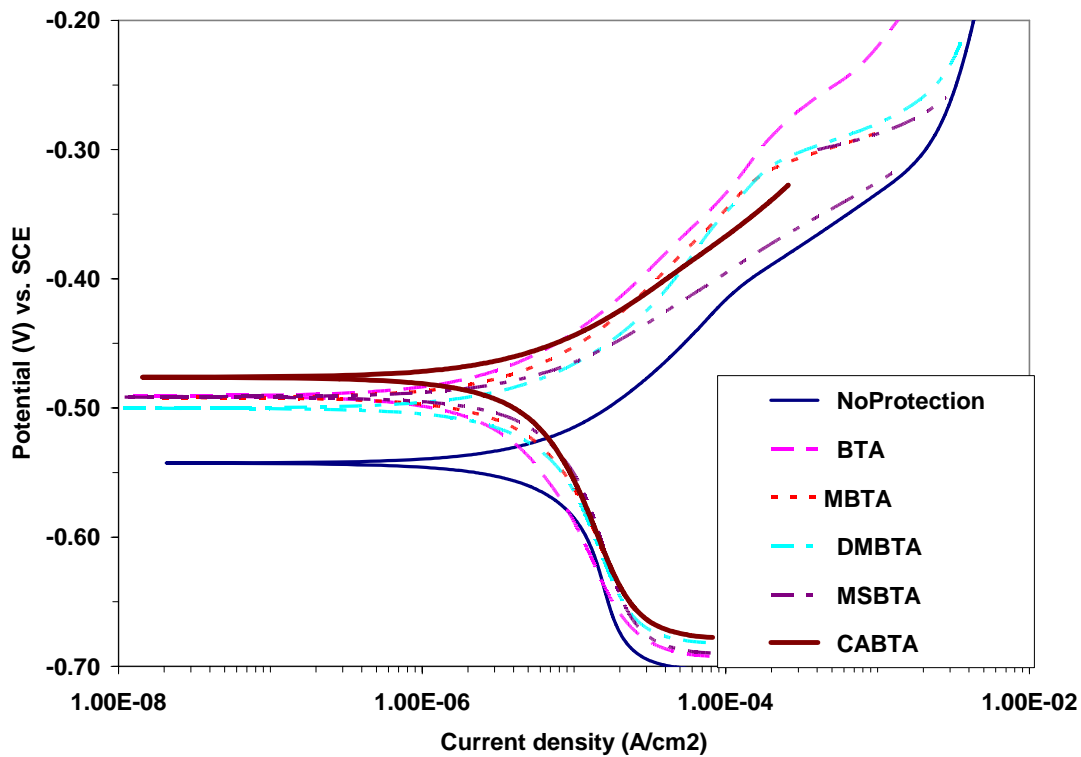


Figure (3): Potentiodynamic polarization curves of steel in SCP solutions under carbonation attack with and without pickling protection system.

## RESULTS

### Potentiodynamic Polarization Results

Figure (2) shows a typical schematic diagram of potentiodynamic polarization curve of steel in SCP solution, and the corrosion potential,  $E_{corr.}$ , at which both the anodic and cathodic currents are equal. The corrosion currents and corrosion rates of each protection systems were calculated using the Tafel extrapolation technique (Jones, 1996). The polarization results of control (blank) solutions are presented in Table (2), where blank 1 solution was SCP solution representing the normal concrete, and blank 2 solution was the SCP solution with pH=8, representing severe carbonation attack. The effectiveness of each protection system and the polarization curves for each BTA derivative will be shown below. Because the carbonation attack always initiates uniform corrosion in the steel of reinforced

concrete, the resistance to carbonation attack is measured through the reduction in corrosion rates.

### Concrete under Carbonation Attack with Pickling Protection System

The idea of the pickling protection system was to incubate the steel specimens in BTA derivatives saturated with  $\text{Ca}(\text{OH})_2$ , so that a protective layer may build and coat the steel surface more effectively. Therefore, when the pretreated steel is exposed to corrosion conditions, the layer coated over the steel surface will protect it against the severe environment. Figure (3) shows the polarization curves in blank 2 solution of steel with and without pickling pretreatment. The steel was pretreated in 0.005 M concentration of BTA derivatives saturated with  $\text{Ca}(\text{OH})_2$  for 15 hours. All of the BTA derivatives improved the corrosion resistance by moving the corrosion potential to more noble potential. Also, Table

(3) shows that high protection efficiency was achieved with most of the BTA derivatives used.

### Concrete under Carbonation Attack with Inhibition Protection System

The BTA derivatives with 0.005 M concentration were used as inhibitors. These were added to the SCP solutions before the polarization tests began. Figure (4)

shows the polarization curves of steel in blank 2 solution and blank 2 with 0.005 M concentration of different BTA derivatives as an inhibitor. The presence of DMBTA or CABTA moved the corrosion potential to more noble potential. Also, as shown in Table (4), MBTA, DMBTA, and MSBTA reduced the corrosion rate with a protection efficiency of around 85%.

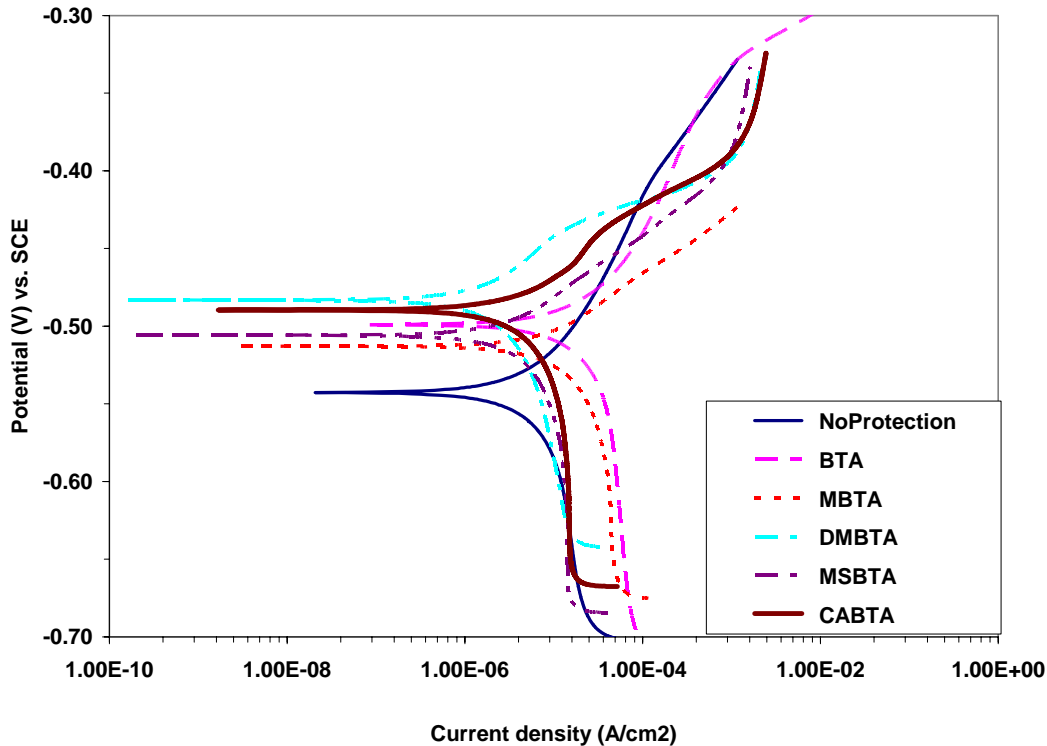


Figure (4): Potentiodynamic polarization curves of steel in SCP solutions under carbonation attack with and without inhibition protection system.

### EIS Results

The schematic diagram of Nyquist plot and the corresponding Randles circuit for steel in SCP solution are shown in Figure (5) where the x-axis is the real impedance,  $Z'$ , and the y-axis is the negative imaginary impedance,  $Z''$ . The solution resistance,  $R_s$ , can be determined by reading the real-axis value at the high frequency intercept; the film resistance,  $R_f$ , and charge transfer resistance,  $R_{ct}$ , can be estimated by extrapolation of the semicircle Nyquist plot to low frequencies

produced real-axis intersection values as shown in Figure (5). The impedance diagrams obtained in the investigations were not perfect semicircles due to frequency dispersion (Ravichandran et al., 2004; Selvi et al., 2003). The capacitance of interfacial reaction,  $C_i$ , was obtained according to the formula:

$$C_i = \frac{1}{\omega_{\max} (R_f + R_{ct})}, \quad \omega_{\max} = 2\pi f_{z''_{\max}} \quad (2)$$

where  $f_{z''_{\max}}$  is the frequency at which the imaginary



impedance is maximum. The efficiency of each protection system and the EIS results for each BTA derivative are discussed below.

**Concrete under Carbonation Attack with Pickling Protection System**

The corrosion behavior of steel in SCP under carbonation attack was investigated after pickling the

steel in saturated calcium hydroxide containing 0.005 M BTA derivative for 15 hours. Nyquist diagrams for steel in SCP solution under carbonation attack with and without pickling protection system are shown in Figure (6) and the impedance parameters of EIS tests are summarized in Table (5). The results showed that the efficiency of pickling protection system of BTA derivatives was around 40%.

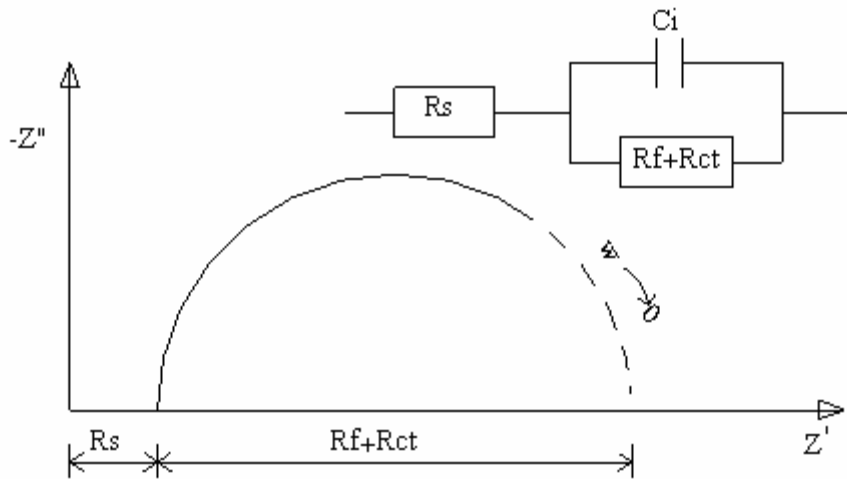


**Figure (5): Schematic diagram of Nyquist plot and equivalent circuit for steel in SCP solution.**

**Concrete under Carbonation Attack with Inhibition Protection System**

The corrosion behavior of steel in SCP under carbonation attack was investigated in the presence of BTA derivatives with 0.005 M concentration as inhibitors by EIS. Nyquist diagrams for steel in SCP solution under carbonation attack with and without inhibition protection system are shown in Figure (7) and the impedance parameters of EIS tests are summarized in Table (6). The results showed that the efficiency of inhibition protection system of BTA derivatives exceeds 60%.

**DISCUSSION**

The results of the potentiodynamic polarization tests with the pickling protection system indicate that all BTA derivatives tested can operate as good coating materials

against corrosion with the corrosion potential,  $E_{corr}$ , shifting to more noble values (as seen in Figure 3). The use of BTA derivatives as pickling protection systems improves the corrosion resistance by shifting the polarization curves to more noble potentials. Moreover, the steel corrosion rates become lower than the ones obtained for the specimen without protection (blank 2), and the protection efficiency exceeds 60%.

The results of the potentiodynamic polarization tests with the inhibition protection system also indicate that the BTA derivatives can operate as good inhibitors. The improvement in the corrosion resistance is demonstrated by the shifting of the polarization curves to more noble potential. Also, the steel corrosion rates become lower than those of the specimen without protection (blank 2), and the protection efficiency reaches up to 85%.

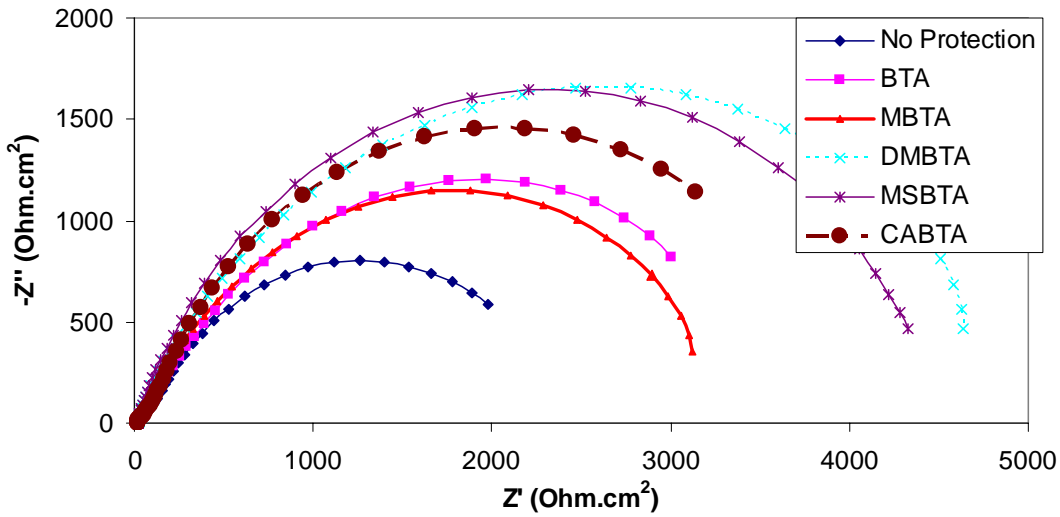


**Figure (6): Nyquist diagrams for steel in SCP solutions under carbonation attack with and without pickling protection system.**

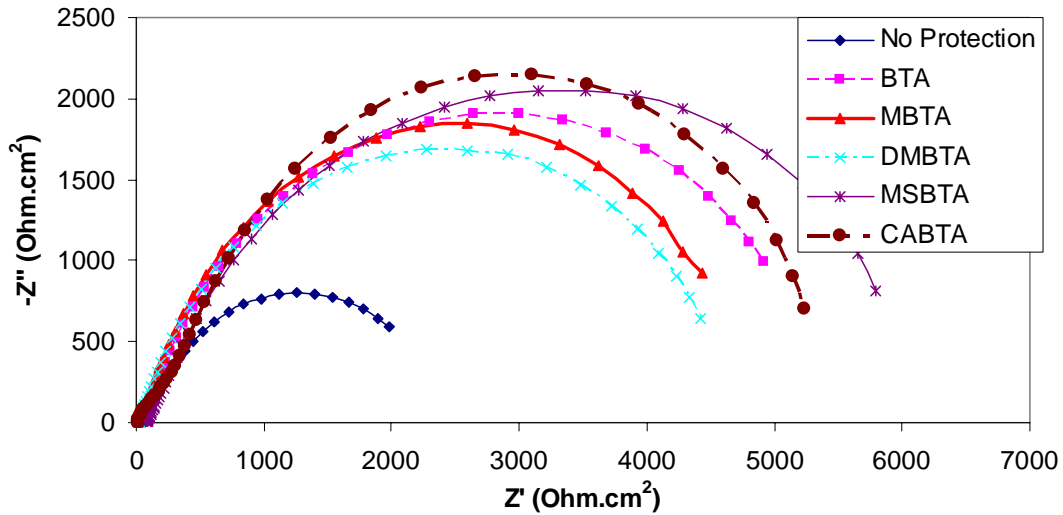


**Figure (7): Nyquist diagrams for steel in SCP solutions under carbonation attack with and without inhibition protection system.**

The EIS spectra results are shown in the Nyquist diagram in Figures (6 and 7). Both protection systems show a large increase in the film resistance,  $R_f$ , and charge transfer resistance,  $R_{ct}$ , and a reduction in the capacitance of interfacial reaction,  $C_i$ , (Tables 5 and 6) which is an indication of the improvement of steel

corrosion resistance and thus a reduction in the corrosion rate. The inhibition system has higher efficiency as compared to the pickling protection. This may be due to the fact that the film formed in pickling was partially deteriorated under the low pH value. In addition, in the inhibition system, the availability of BTA's in the

solution helps building a more continuous film on the steel surface. The small changes in the solution resistances,  $R_s$ , in Table (5) is due to small variation in the position of the Luggin bridge within each test.

Both the EIS spectra and the polarization tests demonstrate the formation of a protective film on the steel surface which increases the corrosion resistance and decreases the corrosion rate; therefore the formation of the protective film is responsible for the enhanced protection and reduction in the corrosion rate. Similar results were obtained with this system under chloride attack (Sheban et al., 2007). Sheban et al. (2007) showed that the protective film consists of a complex of steel and BTA derivatives using FTIR spectra.

### CONCLUSIONS

The tendency of steel to corrode in concrete is well known. Whereas in the past the main concern was on the performance of the concrete itself, here, we tried to improve the protection of the steel in the surrounding concrete. Two protection systems, inhibition and pickling, with five different BTA derivatives were tested in SCP solutions to illustrate the effectiveness of these systems. The SCP solutions simulated severe environmental conditions under carbonation attack,

which is one of the main causes of corrosion of steel in concrete structures. The following points can be concluded from this research:

1. The BTA based inhibition protection system showed a reduction in the corrosion rate and a shifting in the corrosion potential to more noble potentials for the steel specimen in the solution simulated carbonated concrete.
2. The BTA derivatives operated as good inhibitors in simulated concrete under carbonation attack.
3. The protection in both systems was due to the adsorption of BTA derivatives on the steel surface. These act by building a barrier layer around the steel, protecting the steel against corrosion.
4. The electrochemical impedance spectroscopy shows that the resistance is increased and the capacitance is decreased due to the steel-BTA film formation.
5. BTA derivatives provided a good protection for the steel in SCP solutions, and this indicates their applicability in reinforced concrete structures. However, tests using reinforced concrete samples are required to study if there is an interaction between steel, BTA derivatives and concrete constituents, e.g., sand, gravel, cement and chemical admixtures.

### REFERENCES

- Abdullah, A.M., Al-Kharafi, F.M. and Ateya, B.G. 2006. *Scripta Materialia*, 54, 1673.
- Alonso, C., Andrade, C., Argiz, C. and Malric, B. 1996. *Cement and Concrete Research*, 26, 405.
- Andrade, C., Alonso, C. and Gonzalez, J.A. 1986. *Cement, Concrete and Aggregates*, 8, 110.
- Bastidas, D.M. 2006. *Surface and Interface Analysis*, 38, 1146.
- Batis, G., Rakanta, E., Theodoridis, B., Sideris, K.K., Psomas, K. and Barvari, X. 2003. Influence of N,N'-Dimethylaminoethanol Corrosion Inhibitor on Carbonation and Chloride-Induced Corrosion of Steel, *ACI Special Publication*, SP217-31.
- Benture, A., Diamond, S. and Berke, N.S. 1997. *Steel Corrosion in Concrete*, E and FN Spon, London, UK.
- Burge, T.A. 2000. Surface Applied Corrosion Inhibitor, *ACI Special Publication*, SP193-24.
- Haque, M.N. and Kawamura, M. 1993. *ACI Materials Journal*, 89, 41.
- Hartt, W.H., Powers, R.G., Leroux, V. and Lysogorski, D.K. 2004. Critical Literature Review of High-Performance Corrosion Reinforcements in Concrete Bridge Applications, FHWA-HRT-04-093, Office of Infrastructure Research and Development, Federal

- Highway Administration, McLean, VA.
- Hosseini, M.G., Arshadi, M.R., Shahrabi, T. and Ghorbani, M. 2003. *I.J.E.Transaction B*, 16, 255.
- Jones, D.A. 1996. *Principles and Prevention of Corrosion*, Prentice-Hall, Inc., Upper Saddle River, NJ.
- Montemor, M.F., Cunha, M.P., Ferreira, MG. and Simoes, A.M. 2002. *Cement and Concrete Composites*, 24, 45.
- Ravichandran, R., Nanjundan, S. and Rajendran, N. 2004. *Journal of Applied Electrochemistry*, 34, 1171.
- Ravichandran, R., Nanjundan, S. and Rajendran, N. 2004. *Applied Surface Science*, 236, 241.
- Saremi, M. and Mahallati, E. 2002. *Cement and Concrete Research*, 32, 1915.
- Sawada, S., Page, C.L. and Page, M.M. 2005. *Corrosion Science*, 47, 2063.
- Selvi, S.T., Raman, V. and Rajendran, N. 2003. *Journal of Applied Electrochemistry*, 33, 1175.
- Sheban, M., Abu-Dalo, M., Ababneh, A. and Andreescu, S. 2007. *Anti-Corrosion Methods and Materials*, 54, 135.
- Trabanelli, G., Monticelli, C. and Grassi, V. and Frignani, A. 2005. *Cement and Concrete Research*, 35, 1804.
- Xi, Y. and Ababneh, A. 2000. Proc.of the *International Symposium on High Performance Concrete: Workability, Strength and Durability*, Hong Kong and Shenzhen, China, 181.
- Zhang, D.Q., Gao, L.X. and Zhou, G.D. 2006. *Applied Surface Science*, 252, 4975.